Trapped-ion realization of Einstein's recoiling-slit experiment

Robert S. Utter and James M. Feagin*
Department of Physics, California State University-Fullerton, Fullerton, California 92834, USA
(Received 10 July 2006; revised manuscript received 9 October 2006; published 13 June 2007)

We analyze photon scattering by a harmonically trapped ion using two-port interferometry of the scattered photon and coherent-state measurement of the ion's external recoil motion. We examine how the coherent-state measurement could be used to mimick both momentum and position ion measurements and thus a modern realization of Wootters and Zurek's pioneering analysis of Einstein's historic recoiling-slit gedanken experiment. To quantify the photon-path which-port information cached in the recoiling ion and the underlying wave-particle duality, we evaluate the ion-state trace distance and distinguishability.

DOI: 10.1103/PhysRevA.75.062105 PACS number(s): 03.65.Ta, 03.75.Dg, 32.80.Lg

I. INTRODUCTION

Some time ago, Wootters and Zurek [1] revisited the Einstein recoiling-slit gedanken experiment to analyze Young's double-slit interferometry to include in detail the photon which-path information stored in the recoiling entrance slit. They assumed an entrance slit cut into a spring-mounted plate that could be treated as a quantum oscillator under the action of a passing photon. They then considered alternative position and momentum measurements of the plate and the effect of the measurements on the photon interference. Wootters and Zurek thus exploited the underlying photon-plate entanglement to formulate quantitative statements about wave-particle duality, and their work became one of the first major publications on the subject.

Here, we consider photon scattering by a trapped ion as a modern realization of Wootters and Zurek's quantum analysis of the recoiling-slit experiment. While a harmonically trapped ion provides a perfect quantum realization of a spring-mounted plate and entrance slit, we find that a coherent-state measurement of the recoiling ion, besides likely having experimental advantages, can mimic both position and momentum measurements of the ion in full analogy with Wootters and Zurek. One readily identifies the resulting photon fringe visibility as the overlap of recoil-ion marker states describing a photon scattered towards one or the other slit. When the overlap vanishes, the direction of the scattered photon can in principle be determined via the photon-ion entanglement by a measurement of the recoil ion, blocking an interference effect. On the other hand, when the overlap is perfect the interference is as well, and neither the direction of the recoiling ion nor of the scattered photon is discernible. The intermediate stage of duality characterized by moderate overlap continues to warrant further study.

Trapped-ion interferometry has advanced extraordinarily in recent years. Young's fringes formed by photons scattered by a pair of harmonically trapped $^{198}Hg^{+}$ ions have been observed and analyzed in detail by Wineland, Itano, and coworkers at NIST-Boulder [2]: Coherent and squeezed states [3] as well as double-humped superpositions of displaced coherent states [4] of (external) motion of a harmonically trapped $^{9}Be^{+}$ ion have been engineered by Monroe, Meekhof, Wineland, and co-workers. Entanglement analogous to the photon-ion external-motion entanglement we consider here has been observed between the *internal* states of a trapped ion and a polarization-analyzed fluorescence photon by Blinov, Monroe, and co-workers at Michigan [5]. In a recent tour de force, quantum teleportation between three trapped ions has been achieved by Wineland, Itano, and co-workers at NIST [7] and independently by Blatt and co-workers at the Universität Innsbruck [6].

We introduce an impulse approximation to separate the internal states of the ion that scatter the photon from the ion's external c.m. motion and to ensure momentum conservation explicitly. Our description is based on photon-ion *momentum* entanglement and is readily linked to the Wootters and Zurek analysis. Because of the improved detection efficiency, we consider basic two-port photon interferometry with a symmetric beam splitter in place of the Young's double-slit interferometry that Wootters and Zurek considered. The work we describe here is an outgrowth of our related considerations of reaction and fragmentation interferometry [8,9]. We have found [10] the impulse approximation to be a useful tool in describing and analyzing a variety of decoherence effects involving double-humped center-of-mass (c.m.) states of a single atom or ion inside an atom or trapped-ion interferometer, including a particularly compact derivation of the ion-pair Young's interference observed at NIST [2].

We have organized the paper as follows. In the next section, we apply the impulse approximation to describe the photon scattering and ion recoil and thus to describe the photon-ion entanglement when the photon is detected by two-port interferometry. In Sec. III, we derive photon-ion joint detection probabilities generally but in a form that facilitates comparison with Wootters and Zurek. In Sec. IV, we specialize to position and momentum measurements of the ion to connect explicitly with Wootters and Zurek's discussion, and in Sec. V we derive form identical results using coherent-state measurement of the recoiling ion. In Sec. VI, we examine quantitatively how reliably the photon path can be predicted for a given fringe visibility by evaluating the trace distance and the distinguishability. We conclude with a short summary in Sec. VII.

*Electronic address: jfeagin@fullerton.edu

II. PHOTON-ION ENTANGLEMENT

We consider an incident photon $\mathbf{k}_\gamma$ resonantly scattered by a single trapped-ion target, as depicted in Fig. 1. We assume for simplicity the photon encounter is impulsive and that the ion's external center-of-mass (c.m.) motion is described throughout the collision by the initial wave function $g_0(\mathbf{C})$ with $\mathbf{C}$ the c.m. position. Then, the asymptotic photon-ion scattered wave in the impulse approximation is given by [11] (see also [10])

$$\psi \sim \frac{e^{ikr}}{r} f_\gamma(\mathbf{k}) e^{i\mathbf{q}\cdot\mathbf{C}} g_0(\mathbf{C}), \tag{1}$$

where $\mathbf{k} \equiv k\hat{\mathbf{r}}$, $\mathbf{q} \equiv \mathbf{k}_\gamma - \mathbf{k}$, and $f_\gamma(\mathbf{k})$ is the resonance fluorescence amplitude. Thus, $\hbar\mathbf{q}$ is the momentum transfer to the target by the scattered photon and $e^{i\mathbf{q}\cdot\mathbf{C}}$ the corresponding momentum boost of the target external state once a photon detection direction $\hat{\mathbf{r}}$ has been selected [12]. The impulse approximation disconnects the target's external motion during the scattering and allows the photon scattering amplitude involving the ion's internal states to be factored from the full scattering amplitude. Therefore, $|f_\gamma(\mathbf{k})|^2$ is the resonance fluorescence cross section for *free-atom* scattering.

As also depicted in Fig. 1, we consider two-port detection interferometry of the scattered photon. We thus select a superposition of asymptotic waves from Eq. (1) corresponding to photon scatter towards one or the other entrance ports along $\mathbf{k}_+$ or $\mathbf{k}_-$. If for simplicity we consider only dipole transitions and photons linearly polarized perpendicular to the plane of the interferometer, we can write this superposition as the photon-ion momentum entangled state

$$|\chi\rangle = 2^{-1/2}(|\mathbf{k}_+\rangle|\mathbf{q}_+\rangle + |\mathbf{k}_-\rangle|\mathbf{q}_-\rangle), \tag{2}$$

where we have renormalized to a single photon entering the interferometer in state $|\mathbf{k}_+\rangle$ or $|\mathbf{k}_-\rangle$ with the ion recoiling in the corresponding motional state $|\mathbf{q}_+\rangle$ or $|\mathbf{q}_-\rangle$. Thus, $\langle\mathbf{r}|\mathbf{k}_\pm\rangle = e^{i\mathbf{k}_\pm\cdot\mathbf{r}} = e^{ikr}$ are the asymptotic photon plane waves, while $\langle\mathbf{C}|\mathbf{q}_\pm\rangle \equiv e^{i\mathbf{q}_\pm\cdot\mathbf{C}} g_0(\mathbf{C})$ are the corresponding wave functions of the recoiling ion in the impulse approximation and thus define the scattering *form factors*

$$F_{m\pm} \equiv \langle g_m|\mathbf{q}_\pm\rangle = \langle g_m|e^{i\mathbf{q}_\pm\cdot\mathbf{C}}|g_0\rangle, \tag{3}$$

where the states $\langle g_m|$ describe the measurement of the ion's external c.m. motion. If one can measure $|\mathbf{q}_+\rangle$ or $|\mathbf{q}_-\rangle$ cleanly, one can determine with certainty which port *A* or *B* the photon enters, and one also refers to the ion-recoil *marker* states $|\mathbf{q}_\pm\rangle$.

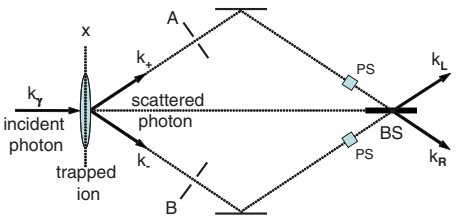

FIG. 1. (Color online) Incident photon with momentum $\hbar\mathbf{k}_\gamma$ scattered by a linearly trapped ion towards the entrance ports *A* and *B* of an interferometer with beam splitter (BS) and phase shifters (PS).

We thus mostly ignore in our analysis the internal electronic states of the ion and simply assume they constitute a two-level system with an upper (resonant) state and a single lower state, for example, the pair of states used in the Doppler cooling and for the quantum-jump measurements of trapped ions. The scattered photon momentum $\hbar\mathbf{k}$ and therefore the ion momentum transfer $\hbar\mathbf{q}$ depend in principle on the final c.m. energy of the ion E_m via energy conservation. However, $\Delta E_m = E_m - E_0 \sim \hbar^2 q^2/2M$ with M the ion mass, so that we can assume $k = k_\gamma$ to good approximation. This assumption is not unrelated to the validity of the impulse approximation which assumes the time development of the external motion is switched off or frozen during the fluorescence scattering, so that a rough criterion for the validity of Eq. (1) is to require the fluorescence lifetime to remain small compared to the excitation time of the external motion so that, say, $\Delta E_m/\hbar\gamma_r \ll 1$, where γ_r is the decay rate of the resonance.

For example, in the case of the ion-pair Young's fringes observed at NIST [2], the (single-ion) recoil energy from the $\lambda_\gamma = 194$ nm scattered photons is approximately $\Delta E_m \sim h \times 26.7$ kHz compared to a resonance width of $\hbar\gamma_r \simeq h \times 70$ MHz, so that $\Delta E_m/\hbar\gamma_r < 0.001$. By comparison, the trap frequency was $\nu_x/2\pi \simeq 1$ MHz corresponding to a period of oscillation a few hundred times longer than the resonance lifetime, viz. $2\pi/\nu_x \simeq 440/\gamma_r$. Likewise, the natural linewidth of the $^9Be^+$ fluorescence used to observe various nonclassical states of ion motion [3,4] is $\hbar\gamma_r \simeq h \times 19.4$ MHz and therefore ~86 photon recoils wide so that $\Delta E_m/\hbar\gamma_r \sim 0.01$. By comparison, the trap frequency was $\nu_x/2\pi \simeq 11.2$ MHz corresponding to a period of oscillation $\tau = 2\pi/\nu_x$ some 11 times longer than the resonance lifetime, viz. $\tau \simeq 10.9/\gamma_r$.

III. PHOTON-ION JOINT PROBABILITIES

We assume our photon interferometer consists of a pair of phase shifters and a symmetrical beam splitter, as depicted in Fig. 1, and thus with sufficient generality represent our photon measurements with the states

$$\langle\mathbf{k}_{L,R}| = 2^{-1/2}(e^{-i\phi/2}\langle\mathbf{k}_+| \pm e^{+i\phi/2}\langle\mathbf{k}_-|), \tag{4}$$

where ϕ is a phase angle set by the phase shifters, which we shall assume can be varied. As also depicted in Fig. 1, $\mathbf{k}_{L,R}$ represent left (L) and right (R) exit ports of the beam splitter as viewed from the ion out along the axis of the interferometer. Then, assuming a coincidence measurement of the ion's external c.m. motion described by $\langle g_m|$, we thus calculate joint photon-ion detection probabilities according to

$$I_{mL,R}(\phi) = |\langle\mathbf{k}_{L,R}, g_m|\chi\rangle|^2 = \frac{1}{2}[I_m \pm 2I_{m+}^{1/2} I_{m-}^{1/2} \cos(\phi - \Delta\varphi_m)], \tag{5}$$

where we have introduced the joint *which-port* probabilities

$$I_{m\pm} = |\langle \mathbf{k}_{\pm}, g_m|\chi\rangle|^2 = \frac{1}{2}|F_{m\pm}|^2 \tag{6}$$

that determine the likelihood via the form factors from Eq. (3) that the photon scatters towards port A ($\mathbf{k}_+$) or port B ($\mathbf{k}_-$) along with finding the ion's c.m. described by $\langle g_m|$, so that $I_m = I_{m+} + I_{m-}$ is the joint probability that the photon enters the interferometer [13]. Also, $\Delta\varphi_m = \varphi_{m+} - \varphi_{m-}$ is the phase difference from $F_{m\pm} = |F_{m\pm}|e^{i\varphi_{m\pm}}$.

To facilitate comparison with Wootters and Zurek, it is convenient to take this a step further and introduce *conditional* probabilities

$$p_{m\pm} = I_{m\pm}/I_m, \tag{7}$$

for hitting port A or port B given the ion c.m. measurement result $\langle g_m|$ so that $p_{m+} + p_{m-} = 1$ [14]. Then, the photon-ion joint probability Eq. (5) can be expressed as

$$I_{mL,R}(\phi) = \frac{1}{2}I_m[1 \pm 2p_{m+}^{1/2}p_{m-}^{1/2}\cos(\phi - \Delta\varphi_m)]. \tag{8}$$

Note, $I_{mL}(\phi) + I_{mR}(\phi) = I_m$, the probability the photon enters the interferometer, independent of ϕ.

Equation (8) generalizes the Einstein recoiling-slit experiment to arbitrary ion measurement states $\langle g_m|$. These joint probabilities describe partial interference patterns of ensembles of photons correlated to particular measurements performed on the ion. What particular partial interference pattern is observed depends on what measurement is performed on the ion. We nevertheless readily obtain the total photon interference pattern when the ion c.m. measurement results are ignored by summing Eq. (8) over all $\langle g_m|$. Invoking closure, one sees that $\Sigma_m|F_{m\pm}|^2 = 1$ so that $\Sigma_m I_{m\pm} = 1/2$ and $\Sigma_m I_m = 1$. On the other hand, the interference terms (cross terms) that contribute to Eq. (5) define a fringe sharpness (or contrast) factor [cf. Eq. (3)]

$$\sum_m F_{m+}^* F_{m-} = \langle \mathbf{q}_+|\mathbf{q}_-\rangle = \langle g_0|e^{-i\Delta\mathbf{q}\cdot\mathbf{C}}|g_0\rangle \equiv S, \tag{9}$$

where $\Delta\mathbf{q} = \mathbf{q}_+ - \mathbf{q}_-$ is the momentum fuzziness transferred to the ion by a photon entering one or the other port. Taking $S \equiv |S|e^{i\varphi_S}$, we thus obtain

$$I_{L,R}(\phi) = \sum_m I_{mL,R}(\phi) = \frac{1}{2}[1 \pm \mathcal{V}\cos(\phi + \varphi_S)], \tag{10}$$

with a fringe visibility

$$\mathcal{V} \equiv |S| = |\langle \mathbf{q}_+|\mathbf{q}_-\rangle|. \tag{11}$$

If g_0 has definite parity, S is real valued and $\varphi_S \equiv 0$.

We thus extend to arbitrary ion measurements Wootters and Zurek's observation that the total interference pattern (the sum of the partial interference patterns) when the ion c.m. motion is ignored is always the same and characterized by the overlap $S = \langle \mathbf{q}_+|\mathbf{q}_-\rangle$ of the kicked-ion states. Note now $I_L(\phi) + I_R(\phi) = 1$.

IV. WOOTTERS AND ZUREK

To connect with Wootters and Zurek, we consider a linearly trapped ion oscillating along the x axis in a harmonic oscillator ground state $\langle x|g_0\rangle = \psi_0(x)$ with width parameter $\Delta_x = \sqrt{\hbar/2M\nu_x}$, the rms size of the wave packet, for an ion of mass M and a trap with frequency ν_x. We also assume an incident photon propagation direction aligned along the axis of the interferometer and perpendicular to the trap axis, as depicted in Fig. 1, so that $q_{x\pm} = \pm\frac{1}{2}\Delta q_x$.

If, following Wootters and Zurek, we now consider a position measurement of the ion described by $\langle g_m| \equiv \langle x|$, the scattering form factor from Eq. (3) evaluates trivially to $F_{x\pm} = e^{\pm i\Delta q_x x/2}\psi_0(x)$ and the results of the previous section are readily applied. Since ψ_0 is real valued, the phase shift in Eq. (8) is given by $\Delta\phi_x = -\Delta q_x x$, and the joint which-port probabilities from Eq. (6) for the photon to enter one or the other port are seen to be equal,

$$I_{x\pm} = \frac{1}{2}|F_{x\pm}|^2 = \frac{1}{2\sqrt{2\pi}\Delta_x}e^{-x^2/2\Delta_x^2}, \tag{12}$$

so that the conditional which-port probabilities from Eq. (7) are also equal, namely, $p_{x\pm} = 1/2$. Thus, the joint photon-ion intensity from Eq. (8) becomes

$$I_{xL,R}(\phi) = \frac{1}{2}I_x[1 \pm \cos(\phi - \Delta q_x x)], \tag{13}$$

which predicts perfect fringes with unit fringe visibility but shifted in phase by $-\Delta q_x x$, as deduced by Wootters and Zurek [15]. Here, $I_x = I_{x+} + I_{x-}$ is the probability that the photon enters the interferometer when the ion c.m. is found at position x. It amounts to a Gaussian modulation factor defined by Eq. (12) that derives from the finite width of the ion c.m. initial wave packet and is analogous to a single-slit diffraction contribution to the two-slit interference.

If, following Einstein's suggestion, we consider instead a measurement of the ion's recoil momentum $\hbar K$ described by $\langle g_m| \equiv \langle K|$ to track the photon's path, we readily evaluate the scattering form factor from Eq. (3) as $F_{K\pm} = \tilde{\psi}_0(K \mp \frac{1}{2}\Delta q_x)$, where $\tilde{\psi}_0(K)$ designates the ion's ground-state *momentum* wave function (Fourier transform of ψ_0) and is also real valued. One then finds the joint which-port probabilities from Eq. (6) to be

$$I_{K\pm} = \frac{1}{2}|F_{K\pm}|^2 = \frac{\Delta_x}{\sqrt{2\pi}}e^{-2(K \mp \Delta q_x/2)^2\Delta_x^2}, \tag{14}$$

so that the conditional probabilities from Eq. (7) are now given by

$$p_{K\pm} = \frac{1}{2}[1 \pm \tanh(2K\Delta q_x\Delta_x^2)]. \tag{15}$$

The joint photon-ion intensity from Eq. (8) thus becomes instead

$$I_{KL,R}(\phi) = \frac{1}{2} I_K[1 \pm \mathrm{sech}(2K\Delta q_x \Delta_x^2)\cos\phi], \tag{16}$$

which is again equivalent to Wootters and Zurek's momentum measurement result and predicts smeared but unshifted fringes [16]. Here, $I_K = I_{K+} + I_{K-}$.

One thus verifies that the partial interference patterns defined by the joint photon-ion probabilities Eqs. (13) and (16) correspond to particular ensembles of photons correlated to either position or momentum measurements performed on the ion. Nevertheless, the total interference pattern ignoring ion measurement results is always the same. One finds from Eq. (9) that

$$S = \langle \mathbf{q}_+ | \mathbf{q}_- \rangle = e^{-\Delta q_x^2 \Delta_x^2/2} \tag{17}$$

is real valued (the ground state has definite parity) so that the photon interference from Eq. (10) becomes

$$I_{L,R}(\phi) = \int dx\, I_{xL,R}(\phi) = \int dK\, I_{KL,R}(\phi) = \frac{1}{2}(1 \pm \mathcal{V}\cos\phi), \tag{18}$$

with fringe visibility $\mathcal{V} = e^{-\Delta q_x^2 \Delta_x^2/2}$, again in agreement with Wootters and Zurek.

We note in passing that $\Delta q_x = 2k_\gamma \sin\frac{1}{2}\theta$ with θ the angular separation of the two entrance ports (the angle between $\mathbf{k}_+$ and $\mathbf{k}_-$) in the plane of the interferometer (see Fig. 1). Also, $\eta_x \equiv k_\gamma \Delta_x$ defines the trap's Lamb-Dicke parameter, so that the fringe visibility

$$\mathcal{V} = e^{-2\eta_x^2 \sin^2(\theta/2)} \tag{19}$$

is essentially unity in the Lamb-Dicke limit $\eta_x \ll 1$.

V. WOOTTERS AND ZUREK VIA COHERENT-STATE MEASUREMENT

We consider now a more general coherent-state measurement of the ion c.m. described by $\langle g_m| \equiv \langle \beta|$ with β complex valued and therefore by a displaced and kicked oscillator ground state with nonvanishing coordinate and momentum (wave number) expectation values

$$\bar{x}_\beta \equiv 2\Delta_x \,\mathrm{Re}\,\beta, \quad \bar{K}_\beta \equiv \mathrm{Im}\,\beta/\Delta_x, \tag{20}$$

respectively, and with the same ground-state rms size $\Delta_x = \sqrt{\hbar/2M\nu_x}$ introduced in the previous section [17]. Coherent states of trapped ions as well as unitary phase-space displacement of coherent states have been realized in the laboratory [3,4], and coherent-state measurements of the ion's recoil motion may have experimental advantages [18] over the position and momentum measurements analyzed by Wootters and Zurek.

For generality, we will assume the initial state of the trapped ion is also a coherent state $|g_0\rangle = |\alpha\rangle$ with nonvanishing coordinate and momentum (wave number) expectation values

$$\bar{x}_\alpha \equiv 2\Delta_x \,\mathrm{Re}\,\alpha, \quad \bar{K}_\alpha \equiv \mathrm{Im}\,\alpha/\Delta_x, \tag{21}$$

respectively, so that when $\alpha = 0$ then $\langle x | g_0 \rangle = \psi_0(x)$ is just the oscillator ground state we assumed for the Wootters and Zurek analysis in the previous section. Coherent states are remarkably robust and remain coherent not only as they oscillate in time but also under the impulsive momentum kicks we consider here. Assuming the photon scattering takes place suddenly at $t=0$, a straightforward calculation thus gives for the kicked initial state

$$|\mathbf{q}_\pm\rangle = e^{iq_{x\pm}x}|\alpha\rangle = e^{+iq_{x\pm}\Delta_x \mathrm{Re}\,\alpha}|\alpha + iq_{x\pm}\Delta_x\rangle. \tag{22}$$

Because of the underlying Gaussian nature of coherent-state wave functions, the form factors from Eq. (3) can be reduced to Gaussian expressions. We thus obtain (dropping an incidental phase)

$$F_{\beta\pm} = e^{iq_{x\pm}\Delta_x(\mathrm{Re}\,\beta + \mathrm{Re}\,\alpha)} e^{-(\mathrm{Re}\,\beta - \mathrm{Re}\,\alpha)^2/2} e^{-(\mathrm{Im}\,\beta - \mathrm{Im}\,\alpha - q_{x\pm}\Delta_x)^2/2}. \tag{23}$$

Taking as before the incident photon propagation direction along the axis of the interferometer so that $q_{x\pm} = \pm\frac{1}{2}\Delta q_x$, we thus evaluate the joint which-port probabilities from Eq. (6) as

$$I_{\beta\pm} = \frac{1}{2\pi}|F_{\beta\pm}|^2 = \frac{1}{2\pi} e^{-(\mathrm{Re}\,\beta - \mathrm{Re}\,\alpha)^2} e^{-(\mathrm{Im}\,\beta - \mathrm{Im}\,\alpha \mp \Delta q_x \Delta_x/2)^2}, \tag{24}$$

where we have introduced an additional factor of $1/\pi$ to compensate for the overcompleteness of coherent states [19]. We thus ensure that $\int d^2\beta I_{\beta\pm} = 1/2$, viz. equal which-port probabilities when the ion c.m. recoil is ignored [cf. discussion above Eq. (9)].

Then, the conditional which-port probabilities from Eq. (7) are given by

$$p_{\beta\pm} = \frac{1}{2}\{1 \pm \tanh[\Delta q_x \Delta_x(\mathrm{Im}\,\beta - \mathrm{Im}\,\alpha)]\}, \tag{25}$$

independent of Re α and Re β and, in light of the expectation value $\bar{K}_\beta \equiv \mathrm{Im}\,\beta/\Delta_x$ from Eq. (20), are form identical with the Wootters and Zurek momentum-measurement results Eq. (15). The missing factor of two here is an artifact of the underlying Gaussian overlap integrals of the coherent-state wave functions.

Thus, the joint photon-ion intensity from Eq. (8) becomes

$$I_{\beta L,R}(\phi) = \frac{1}{2} I_\beta \{1 \pm \mathrm{sech}[\Delta q_x \Delta_x(\mathrm{Im}\,\beta - \mathrm{Im}\,\alpha)] \times \cos[\phi - \Delta q_x \Delta_x(\mathrm{Re}\,\beta + \mathrm{Re}\,\alpha)]\}, \tag{26}$$

where $I_\beta = I_{\beta+} + I_{\beta-}$.

One therefore mimicks with this result Wootters and Zurek's *position* measurement of the ion's ground state by taking $\mathrm{Im}\,\beta \equiv 0$ and $\alpha \equiv 0$ and introducing the coherent-state expectation value $\bar{x}_\beta$ from Eq. (20) to give

$$I_{\bar{x}_\beta L,R}(\phi) = \frac{1}{2} I_{\bar{x}_\beta}\left[1 \pm \cos\left(\phi - \frac{1}{2}\Delta q_x \bar{x}_\beta\right)\right], \tag{27}$$

which is form identical with Eq. (13) except for the extra factor 1/2 here in the phase shift and the modified overall intensity

$$I_{\bar{x}_\beta} = \frac{1}{\pi} e^{-\bar{x}_\beta^2 \Delta_x^2/4} e^{-\Delta q_x^2 \Delta_x^2/4}. \tag{28}$$

Likewise, one mimicks Wootters and Zurek's *momentum*-measurement result by taking Re $\beta \equiv 0$ and $\alpha \equiv 0$ in Eq. (26) and introducing $\bar{K}_\beta$ from Eq. (20) to give

$$I_{\bar{K}_\beta L,R}(\phi) = \frac{1}{2} I_{\bar{K}_\beta}[1 \pm \mathrm{sech}(\bar{K}_\beta \Delta q_x \Delta_x^2)\cos\,\phi], \tag{29}$$

which is also form identical with Eq. (16) except for the missing factor of 2 here in the fringe visibility function $\mathrm{sech}(\bar{K}_\beta \Delta q_x \Delta_x^2)$ and again a modified overall intensity

$$I_{\bar{K}_\beta} = \frac{1}{2\pi}\left(e^{-(\bar{K}_\beta - \Delta q_x/2)^2 \Delta_x^2} + e^{-(\bar{K}_\beta + \Delta q_x/2)^2 \Delta_x^2}\right). \tag{30}$$

While these joint photon-ion probabilities mimick well enough those of Wootters and Zurek [Eqs. (13) and (16)], neither Eq. (27) nor Eq. (29) integrates to the photon interference result Eq. (18). [20] When ion c.m. measurements are ignored, one must instead integrate over the entire β plane ($\bar{x}_\beta$ and $\bar{K}_\beta$ together). Thus, the photon interference pattern from Eq. (26) integrated over the ion coherent-state measurement results, in analogy with Eq. (18), is given by

$$I_{L,R}(\phi) = \int d^2\beta\, I_{\beta L,R}(\phi) = \frac{1}{2}[1 \pm \mathcal{V}\cos(\phi - 2\Delta q_x \Delta_x\, \mathrm{Re}\,\alpha)], \tag{31}$$

with $\mathcal{V} = e^{-\Delta q_x^2 \Delta_x^2/2}$ and is therefore identical for $\alpha = 0$ to the photon-interference result Eq. (18). Equation (31) also follows directly from Eq. (10) by noting that the fringe sharpness factor from Eq. (9) is given with Eq. (22) by

$$S_\alpha = \langle \alpha | e^{-i\Delta q_x x} | \alpha \rangle = \mathcal{V} e^{-2i\Delta q_x \Delta_x \mathrm{Re}\,\alpha}, \tag{32}$$

which reduces to Eq. (17) when $\alpha = 0$.

The more general $\alpha \neq 0$ initial-state dependence included in Eqs. (31) and (32) instead facilitates averaging over a thermal distribution of initial states, appropriate if the trap is operated in thermal equilibrium at a finite temperature T. The reason being, the density operator describing an initial ensemble of linearly oscillating ions in thermal equilibrium can be represented equivalently in coherent states according to [17,21]

$$\rho_T = \int \frac{d^2\alpha}{\pi} \frac{e^{-|\alpha|^2/\langle n\rangle}}{\langle n\rangle} |\alpha\rangle\langle\alpha|, \tag{33}$$

with $\langle n\rangle = 1/(e^{\hbar\nu_x/k_B T} - 1)$ the average oscillator-state occupancy (Planck distribution) at temperature T. It then follows, the photon interference pattern Eq. (31) averaged over a thermal distribution of ion initial states $|\alpha\rangle$ is given by

$$\langle I_{L,R}(\phi)\rangle \equiv \int \frac{d^2\alpha}{\pi} \frac{e^{-|\alpha|^2/\langle n\rangle}}{\langle n\rangle} I_{L,R}(\phi) = \frac{1}{2}[1 \pm \mathcal{V}_T \cos\,\phi], \tag{34}$$

with $\mathcal{V}_T = \mathcal{V}^{\coth(\hbar\nu_x/2k_B T)}$ and $\mathcal{V}$ the visibility obtained in Eqs. (18) and (31). In a similar fashion (see also [22]), the fringe sharpness factor from Eq. (32) thermally averaged is found to be $\langle S_\alpha\rangle = \mathcal{V}_T$ and thus defines a Debye-Waller factor [21] for the linearly trapped ion which when inserted into Eq. (10) verifies Eq. (34). Thus, a thermal distribution with $k_B T > \hbar\nu_x$ further reduces the fringe visibility, and in the high temperature limit $\coth(\hbar\nu_x/2k_B T) \sim 2k_B T/\hbar\nu_x$. Analogous results have been obtained and observed by Wineland, Itano, and co-workers in Ref. [2] in their experiments with Young's fringes formed by light scattered from a trapped-ion pair in thermal equilibrium.

VI. WHICH-PORT DISTINGUISHABILITY

In order for the photon phase relations characterizing the system entanglement $|\chi\rangle$ in Eq. (2) to remain accessible for local observation and interference, the ion-recoil marker states $|\mathbf{q}_\pm\rangle$ must overlap. Otherwise, the ion recoil could be cleanly measured and the photon path (which port entered, *A* or *B*) determined unambiguously. If the overlap is perfect the fringes will be perfect with $\mathcal{V} = 1$, and if the overlap vanishes the fringes will as well with $\mathcal{V} = 0$. The ion recoil thus stores information on the port and path taken by the scattered photon. As articulated originally by Wootters and Zurek, the question becomes what goes on between these two extremes. For a given fringe visibility, how reliably can the photon path be predicted?

Although there is no definitive answer to this question, a straightforward estimate is simply to evaluate the difference between our two which-port probabilities from Eq. (6) summed over all possible measurement outcomes, the so-called classical *trace distance* [23], or what Englert has referred to as the which-path *knowledge* [24],

$$D \equiv \sum_m |I_{m+} - I_{m-}|, \tag{35}$$

where we have omitted the usual overall factor 1/2 since recall that our which-port probabilities are normalized such that $\Sigma_m I_{m\pm} = 1/2$. [25]

The value of this measure depends on the ion state observed. For example, we have seen in Eq. (12) if ion position $\langle g_m| = \langle x|$ is measured, $I_{x+} = I_{x-}$ for all x so that $D_x = 0$ no matter what the fringe visibility $\mathcal{V}$ is in Eq. (18). One could just as well coordinate which-port guesses with water drop intervals from a lab faucet.

A better choice would be to follow Einstein's suggestion and measure the ion-recoil momentum instead. Noting from Eq. (14) that $|I_{K+} - I_{K-}|_{K\leq 0} = (I_{K+} - I_{K-})_{K\geq 0}$, one readily finds that

$$D_K = 2\int_0^\infty dK(I_{K+} - I_{K-}) = \mathrm{erf}\left(\frac{\Delta q_x \Delta_x}{\sqrt{2}}\right), \tag{36}$$

with values in the range $0 \leqslant D_K \leqslant 1$ corresponding to $1 \geqslant \mathcal{V} \geqslant 0$ in Eq. (18). In a similar fashion, noting from Eq. (24) that $|I_{\beta+} - I_{\beta-}|_{\mathrm{Im}\,\beta \leqslant \mathrm{Im}\,\alpha} = (I_{\beta+} - I_{\beta-})_{\mathrm{Im}\,\beta \geqslant \mathrm{Im}\,\alpha}$, one finds for a coherent-state measurement that

$$D_\beta = 2\int_{-\infty}^{\infty} d\,\mathrm{Re}\,\beta \int_{\mathrm{Im}\,\alpha}^{\infty} d\,\mathrm{Im}\,\beta (I_{\beta+} - I_{\beta-}) = \mathrm{erf}\left(\frac{\Delta q_x \Delta_x}{2}\right), \tag{37}$$

also with values in the range $0 \leqslant D_\beta \leqslant 1$ and *independent* of the ion-c.m. initial state $|\alpha\rangle$. We plot these quantities in Fig. 2 as a function of $\Delta q_x \Delta_x$ as well as a function of the fringe visibility $\mathcal{V} = e^{-\Delta q_x^2 \Delta_x^2/2}$. The resulting curves are quite similar, although D_β remains smaller than D_K for a given fringe visibility $\mathcal{V}$ (note the extra factor $1/\sqrt{2}$ in the argument of D_β compared to that of D_K). With respect to trace distance, a coherent-state measurement is somewhat inferior to the momentum measurement.

The *independence* of the which-path knowledge Eq. (37) on ion initial state $|\alpha\rangle$ can be traced to the impulsive nature of the light scattering and the Gaussian form of coherent-state overlaps embodied in the which-port probabilities from Eq. (24). Consequently, and perhaps somewhat surprisingly, the distinguishability of the path taken by the scattered photon survives thermal averaging and is independent of the temperature of the target ion, unlike the temperature-dependent reduction in the fringe visibility we established in Eq. (34).

One readily establishes an upper limit on the which-path knowledge for a given fringe visibility $\mathcal{V}$. First, we note that our joint which-port probabilities from Eq. (6) can be reexpressed as

$$I_{m\pm} = \frac{1}{2}|F_{m\pm}|^2 = \frac{1}{2}\mathrm{tr}(P_m \rho_\pm), \tag{38}$$

where we have introduced the density operators $\rho_\pm \equiv |\mathbf{q}_\pm\rangle\langle\mathbf{q}_\pm|$ describing the ion-recoil marking along with the projection operators $P_m \equiv |g_m\rangle\langle g_m|$ describing the ion measurements. The marker states $\rho_\pm$ also define from Eq. (2) the reduced density operator of the ion traced over the photon states $|\mathbf{k}_\pm\rangle$ according to $\rho_q = \mathrm{tr}_k(|\chi\rangle\langle\chi|) = (\rho_+ + \rho_-)/2$. The P_m are positive, orthogonal operators and satisfy the completeness relation $\Sigma_m P_m = 1$.

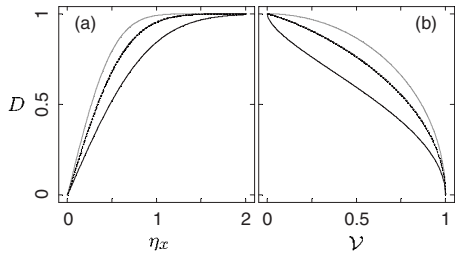

FIG. 2. The which-path knowledge D plotted in (a) as a function of the Lamb-Dicke parameter $\eta_x = k_\gamma \Delta_x$ (taking $\Delta q_x \Delta_x = 2\eta_x$ for $\theta = \pi$) [cf. Eq. (19)] and in (b) as a function of $\mathcal{V} = e^{-\Delta q_x^2 \Delta_x^2/2}$. The middle dotted curve in both plots is D_K from Eq. (36) while the lower solid curve is D_β from Eq. (37). The upper gray curve in both plots is the limiting *quantum* trace distance, or distinguishability $\mathcal{D}$ from Eq. (42).

With no extra effort, we can generalize our which-port probabilities in Eq. (38) to include *nonorthogonal* operators E_m which are nevertheless positive and satisfy $\Sigma_m E_m = 1$. The resulting positive operator-valued measure (POVM) includes the usual projection (von Neumann) measurements as well as our nonorthogonal coherent-state measurements. For example, defining $E_\beta \equiv |\beta\rangle\langle\beta|/\pi$ (cf. Ref. [19]), we thus have

$$I_{\beta\pm} = \frac{1}{2}\mathrm{tr}(E_\beta \rho_\pm) = \frac{1}{2\pi}|F_{\beta\pm}|^2, \tag{39}$$

which we evaluated in Eq. (24). One can thereby reexpress and generalize the trace distance in Eq. (35) as

$$D = \frac{1}{2}\sum_m |\mathrm{tr}[E_m(\rho_+ - \rho_-)]|. \tag{40}$$

An upper bound is now directly accessible by invoking the inequality $|\mathrm{tr}\{E_m(\rho_+ - \rho_-)\}| \leqslant \mathrm{tr}\{E_m|\rho_+ - \rho_-|\}$, which is readily established with the spectral decomposition of $\rho_+ - \rho_-$. [23] Then, with $\Sigma_m E_m = 1$, one has that

$$D \leqslant \mathcal{D} \equiv \frac{1}{2}\mathrm{tr}|\rho_+ - \rho_-|, \tag{41}$$

defining the *quantum* trace difference $\mathcal{D}$, or what Englert [24] referred to as the *distinguishablility* of the ways. [26] Equality $D = \mathcal{D}$ is established in Eq. (41) when the E_m are chosen to project onto the two eigenstates of $\rho_+ - \rho_-$, and a quick calculation determines the corresponding eigenvalue pair $\pm\mathcal{D}$ with

$$\mathcal{D} = \sqrt{1 - |S_\alpha|^2} = \sqrt{1 - \mathcal{V}^2}, \tag{42}$$

using Eq. (32), which is also independent of the ion's initial state $|\alpha\rangle$. This quantity is also plotted in Fig. 2. The resulting *duality* relation $\mathcal{D}^2 + \mathcal{V}^2 = 1$ between the distinguishability of the ways and the fringe visibility derives from the fact we have implicitly assumed our $\rho_\pm$ to be pure states. More generally for mixed initial states, Englert [24] and independently Jaeger, Shimony, and Vaidman [27] have shown that $\mathcal{D}^2 + \mathcal{V}^2 \leqslant 1$. For example, for an ensemble of initial ions in thermal equilibrium, we obtain the special case $\mathcal{D}^2 + \mathcal{V}_T^2 \leqslant 1$ with $\mathcal{V}_T$ defined by Eq. (34). The duality relation has been verified by Dürr, Nonn, and Rempe in atom-interferometer experiments that monitored atom path and *internal*-state entanglement [28] and by Schwindt, Kwiat, and Englert in photon-interferometer experiments that monitored photon path and polarization entanglement. [29]

As a follow-on to the eigenvalue determination and Eq. (42), one obtains the eigenstates of $\rho_+ - \rho_-$ in terms of the ion-recoil marker states $|\mathbf{q}_\pm\rangle$ from Eq. (22) according to

$$|\pm\mathcal{D}\rangle = e^{+i\varphi_S/2}\frac{\sqrt{1\pm\mathcal{D}}}{\sqrt{2}\mathcal{D}}|\mathbf{q}_+\rangle - e^{-i\varphi_S/2}\frac{\sqrt{1\mp\mathcal{D}}}{\sqrt{2}\mathcal{D}}|\mathbf{q}_-\rangle, \quad (43)$$

with $\varphi_S=-2\Delta q_x\Delta_x$ Re α the phase of S_α from Eq. (32). One verifies directly with Eqs. (9) and (32) that $(\rho_+-\rho_-)|\pm\mathcal{D}\rangle = \pm\mathcal{D}|\pm\mathcal{D}\rangle$. These states describe, of course, optimal measurements of the ion's c.m. motion with $\langle g_m| \equiv \langle\pm\mathcal{D}|$ for distinguishing which port the photon scattered into. One thus obtains from Eq. (6), again with Eqs. (9) and (32), the optimum probabilities $I_{(\pm\mathcal{D})+}=(1\pm\mathcal{D})/4$ for photon scattering into port $A(\mathbf{k}_+)$ and $I_{(\pm\mathcal{D})-}=(1\mp\mathcal{D})/4$ into port $B(\mathbf{k}_-)$ independently of the ion's initial state $|\alpha\rangle$. As $\mathcal{D}\to 1$, the ion marker states become effectively orthogonal, $S_\alpha=\langle\mathbf{q}_+|\mathbf{q}_-\rangle \to 0$, and by definition fully distinguishable, and Eq. (43) reduces to simply $|\pm\mathcal{D}\rangle \to \pm e^{\pm i\varphi_S/2}|\mathbf{q}_\pm\rangle$. For $\mathcal{D}=0$, Eq. (43) is not defined, but in that case $S_\alpha=1$ so that the ion marker states fully overlap and are therefore indistinguishable anyway.

Although measurement of these states will undoubtedly prove challenging, similar superpositions of coherent states of trapped-ion external motion have been engineered and observed in Ref. [4]. The optimal marker wave functions $\langle x|\pm\mathcal{D}\rangle$ defined by Eq. (43) evolve in time as double-humped superpositions of the coherent-state wave functions $\langle x|\mathbf{q}_\pm\rangle$ from Eq. (22) and therefore oscillate with a period $2\pi/\nu_x$. To see this, note that coherent states evolve in time according to $|\eta\rangle \to e^{-i\nu_x t/2}|\eta e^{-i\nu_x t}\rangle$. [17] At $t=0$, the instant the photon is scattered by the ion, the two humps defined by $\langle x|\mathbf{q}_\pm\rangle$ coalesce at $\bar{x}_\alpha$ with relative momentum $\hbar\Delta q_x$. A quarter period later at $t=\pi/2\nu_x$, the two humps will have moved to their maximum relative separation $d=2\Delta q_x\Delta_x^2$ with zero relative momentum (cf. also the discussion in [10]). Averaged over a thermal distribution of initial ion states $|\alpha\rangle$, the initial relative momentum $\hbar\Delta q_x$ and the maximum observed separation d of the two humps will remain unchanged, while their average initial position will vanish.

We note in passing that alternative techniques for generating and observing double-humped superpositions of coherent states have been proposed by Zoller, Cirac, and coworkers. [30] The proposal presented by Zeng [31] is also noteworthy in this regard.

VII. DISCUSSION

We have examined photon scattering by a harmonically trapped ion as a modern prototype for Wootters and Zurek's pioneering analysis of Einstein's recoiling-slit experiment. We give the trapped ion the role of the oscillating entrance slit and show how coherent-state measurement could be used to mimick both momentum and position measurements of the ion's external recoil motion and thus to track the which-path marking of the scattered photon. The key results are presented in Secs. V and VI.

The simplicity of our results relies on an impulse approximation to describe the photon scattering and the resulting momentum kick to the ion's external c.m. motion. The characteristic scattering form factors from Eq. (3) allow us to link our approach closely to Wootters and Zurek's discussion while providing a fairly rigorous description that can be generalized to alternative ion-measurement schemes.

To quantify the photon-path which-port information cached in the recoiling ion, we have evaluated the classical trace distance, or which-path knowledge, in Eq. (35) between the joint probabilities from Eq. (6) for scattering the photon into one or the other port and detecting the recoiling ion. We connect in this way with ideas introduced by Wootters and Zurek and refined by Englert to give quantitative meaning to partial which-port marking by the ion when the photon fringe visibility is nonvanishing but less than perfect. One is thus led to consider the quantum trace distance, or distinguishability of the ways, in Eq. (41) as an upper bound on the classical trace distance, and one thereby recovers Englert's duality relation between the distinguishability and the fringe visibility Eq. (42).

While our analysis based on the ion's external c.m. motion is straightforward, the actual experiments we describe remain difficult. The joint photon-ion probability in Eq. (8), which we have evaluated throughout this paper in various detection scenarios, describes photon-ion coincidences with a single trapped-ion target reset to the same initial c.m. state before each photon collision. Thus, unless this ion-reset cycle can be significantly accelerated, the time required to collect meaningful ensembles of scattered photons will likely remain exceptionally long. At the same time, the which-path knowledge of the scattered photon we evaluated in Eq. (37) is seen to be independent of the initial state of the harmonically trapped target ion. The photon path could therefore be tracked and compared with predictions without having to reset the ion's initial state between collisions.

We have begun to examine various information-transfer strategies in the context of trapped-ion interferometry. The ion-recoil state difference $\rho_+-\rho_-$ in Eq. (41) defines an optimum observable of sorts whose eigenstates in Eq. (43) determine optimum ion measurements to maximize the which-path knowledge for a given fringe visibility if only which-port probabilities are accessible experimentally. One can also quantify the photon-path information transfer to the ion's external motion by evaluating the decrease in the ion's Shannon entropy due to the photon scattering for a given fringe visibility. Alternatively, one might wish to avoid the which-port probabilities altogether and introduce instead a POVM to distinguish for a given fringe visibility the state of the ion $|\mathbf{q}_+\rangle$ or $|\mathbf{q}_-\rangle$ some of the time with certainty, but with the tradeoff that some of the tests will yield no information [23,32]. We will compare these alternatives elsewhere.

ACKNOWLEDGMENTS

We appreciate useful input from our colleague Heidi Fearn. This project has been supported by the Chemical Sciences, Geosciences and Biosciences Division of the Office of Basic Energy Sciences, Office of Science, U.S. Department of Energy.

[1] W. K. Wootters and W. H. Zurek, Phys. Rev. D **19**, 473 (1979).

[2] U. Eichmann, J. C. Bergquist, J. J. Bollinger, J. M. Gilligan, W. M. Itano, D. J. Wineland, and M. G. Raizen, Phys. Rev. Lett. **70**, 2359 (1993); W. M. Itano, J. C. Bergquist, J. J. Bollinger, D.J. Wineland, U. Eichmann, and M.G. Raizen, Phys. Rev. A **57**, 4176 (1998).

[3] D. M. Meekhof, C. Monroe, B. E. King, W. M. Itano, and D. J. Wineland, Phys. Rev. Lett. **76**, 1796 (1996).

[4] C. Monroe, D. M. Meekhof, B. E. King, and D. J. Wineland, Science **272**, 1131 (1996).

[5] B. B. Blinov, D. L. Moehring, L.-M. Duan, and C. Monroe, Nature (London) **428**, 153 (2004); E. Polzik, *ibid.* **428**, 129(2004).

[6] M. Riebe, H. Häffner, C. F. Roos, W. Hänsel, J. Benhelm, G. P. T. Lancaster, T. W. Körber, C. Becher, F. Schmidt-Kaler, D. F. V. James, and R. Blatt, Nature (London) **429**, 734 (2004).

[7] M. D. Barrett, J. Chiaverini, T. Shaetz, J. Britton, W. M. Itano, J. D. Jost, E. Knill, C. Langer, D. Leibfried, R. Ozeri, and D. J. Wineland, Nature (London) **429**, 737 (2004).

[8] J. M. Feagin and Si-ping Han, Phys. Rev. Lett. **86**, 5039 (2001); J. M. Feagin and Si-ping Han, *ibid.* **89**, 109302 (2002).

[9] J. M. Feagin, Phys. Rev. A **69**, 062103 (2004).

[10] J. M. Feagin, Phys. Rev. A **73**, 022108 (2006).

[11] M. L. Goldberger and K. M. Watson, *Collision Theory*, (Wiley, New York, 1964), p. 707; N. F. Mott and H. S. W. Massey, *The Theory of Atomic Collisions*, 3rd ed. (Oxford University Press, Oxford, 1965), Vol. 1, p. 91.

[12] We use MKS units throughout and keep $\hbar$ explicit.

[13] When multiplied by $|f_\gamma|^2$ from Eq. (1), $I_{mL,R}(\phi)$ gives the cross section for scattering a photon into the interferometer and finding the ion's external c.m. motion described by $\langle g_m|$.

[14] Note $I_{m\pm}$ gives the joint probability for the occurrence of both $\langle \mathbf{k}_\pm|$ and $\langle g_m|$ conditioned only on the state being $|\chi\rangle$.

[15] Wootters and Zurek in Ref. [1] considered double-slit interferometry with effective momentum kicks $\pm k_0$ and thus corresponding entrance-slit recoil kicks $q_{x\pm}=\mp k_0$, so that $\Delta q_x=-2k_0$ in their notation. Also, our ϕ in Eq. (13) takes the role of $2k_0\xi$ in their expressions.

[16] Along with the notation $\Delta q_x=-2k_0$ (cf. Ref. [15]), Wootters and Zurek used $a^2\equiv 2\Delta_x^2$, so that here our fringe sharpness $\mathrm{sech}(2K\,\Delta q_x\Delta_x^2)=\mathrm{sech}(2a^2K\,k_0)$ is equivalent to theirs. In particular, our ratio of conditional probabilities $p_{K+}/p_{K-}=\exp(4K\,\Delta q_x\Delta_x^2)=\exp(-4a^2\,K\,k_0)$ from Eq. (15) is equivalent to Wootters and Zurek's Eq. (4) in Ref. [1]. See also S. M. Tan and D. F. Walls, Phys. Rev. A **47**, 4663 (1993).

[17] See, for example, K. Gottfried and T-M. Yan, *Quantum Mechanics: Fundamentals*, 2nd ed. (Springer, New York, 2003), and E. Merzbacher, *Quantum Mechanics*, 3rd ed. (Wiley, New York, 1998). We thus take $\langle x|\beta\rangle=e^{-i\,\mathrm{Re}\,\beta\,\mathrm{Im}\,\beta}e^{+ix\,\mathrm{Im}\,\beta/\Delta_x}\psi_0(x-2\Delta_x\,\mathrm{Re}\,\beta)$.

[18] M. Freyberger, Phys. Rev. A **55**, 4120 (1997), and references therein.

[19] One has that $\int d^2\beta|\beta\rangle\langle\beta|=\pi$.

[20] Integration of either Eq. (27) over $\bar{x}_\beta$ or Eq. (29) over $\bar{K}_\beta$ gives a photon interference pattern with visibility $\mathcal{V}^{1/2}$.

[21] David S. Bateman, Subir K. Bose, Binayak Dutta-Roy, and Manoranjan Bhattacharyya, Am. J. Phys. **60**, 829 (1992).

[22] N. D. Mermin, J. Math. Phys. **7**, 1038 (1966).

[23] M. A. Nielsen and I. L. Chuang, *Quantum Computation and Quantum Information* (Cambridge University Press, Cambridge, 2000).

[24] B.-G. Englert, Phys. Rev. Lett. **77**, 2154 (1996); Zeit. f. Naturforschungs **54**, 11 (1999); See also B.-G. Englert and J. A. Bergou, Opt. Commun. **179**, 337 (2000).

[25] We also connect with Englert's *likelihood for guessing the right way* according to $\mathcal{L}\equiv\Sigma_m\max\{I_{m+},I_{m-}\}=(1+D)/2$. See Ref. [24].

[26] This result extends Englert's proof somewhat to include POVM.

[27] G. Jaeger, A. Shimony, and L. Vaidman, Phys. Rev. A **51**, 54 (1995).

[28] S. Dürr, T. Nonn, and G. Rempe, Nature (London) **395**, 33 (1998); Phys. Rev. Lett. **81**, 5705 (1998).

[29] P. D. D. Schwindt, P. G. Kwiat, and B.-G. Englert, Phys. Rev. A **60**, 4285 (1999).

[30] J. F. Poyatos, J. I. Cirac, R. Blatt, and P. Zoller, Phys. Rev. A **54**, 1532 (1996); J. F. Poyatos, J. I. Cirac, and P. Zoller, Phys. Rev. Lett. **77**, 4728 (1996).

[31] H. Zeng, Phys. Rev. A **57**, 388 (1998).

[32] A. Peres, *Quantum Theory: Concepts and Methods* (Kluwer Academic Publishers, Dordrecht, 1995).